

Wave-particle dualism of spiral waves dynamics

I. V. Biktasheva*

CFD Laboratory, Department of Engineering, University of Cambridge, Trumpington Street, Cambridge CB2 1PZ, United Kingdom

V. N. Biktashev†

Department of Mathematical Sciences, Liverpool University, Mathematics & Oceanography Building, Peach Street, Liverpool, L69 7ZL, United Kingdom

(Received 11 July 2002; published 27 February 2003)

We demonstrate and explain a wave-particle dualism of such classical macroscopic phenomena as spiral waves in active media. That means although spiral waves *appear* as nonlocal processes involving the whole medium, they *respond* to small perturbations as effectively localized entities. The dualism appears as an emergent property of a nonlinear field and is mathematically expressed in terms of the spiral waves response functions, which are essentially nonzero only in the vicinity of the spiral wave core. Knowledge of the response functions allows *quantitatively* accurate prediction of the spiral wave drift due to small perturbations of any nature, which makes them as fundamental characteristics for spiral waves as mass is for the condensed matter.

DOI: 10.1103/PhysRevE.67.026221

PACS number(s): 82.40.Bj, 02.60.Cb, 64.60.Ht, 87.10.+e

I. INTRODUCTION

Autowaves are nonlinear waves observed in spatially distributed media of physical, chemical, and biological nature, when wave propagation is supported by a source of energy stored in the medium. In a two-dimensional autowave medium there may exist autowave vortices appearing as rotating spiral waves and thus acting as a sources of periodic waves. Their existence is not due to singularities in the medium but is determined only by development from initial conditions. In a slightly perturbed medium, e.g., spatially inhomogeneous, or subject to time-dependent external forcing, a spiral wave drifts, i.e., its core location and frequency change with time.

The first direct experimental observation of spiral waves in a chemical oscillatory medium, the Belousov-Zhabotinsky reaction [1], triggered a huge amount of interest and activity in the area. Soon after that spiral waves were observed in a rabbit ventricular tissue [2], and later in a variety of other spatially distributed active systems: in chick retina [3], colonies of social ameba [4], cytoplasm of single oöcytes [5], in the reaction of catalytic oxidation of carbon oxide [6], rusting of the steel surface in acid with the air [7], in liquid crystal [8], and laser [9] systems. On a larger scale, there are waves of infectious diseases traveling through biological populations [10,11], and spiral galaxies [12,13].

A common feature of all these phenomena is that they can be mathematically described, with various degrees of accuracy, by “reaction-diffusion” partial differential equations,

$$\partial_t \mathbf{u} = \mathbf{f}(\mathbf{u}) + \mathbf{D} \nabla^2 \mathbf{u} + \epsilon \mathbf{h}, \quad \mathbf{u}, \mathbf{f}, \mathbf{h} \in \mathbb{R}^\ell, \quad \mathbf{D} \in \mathbb{R}^{\ell \times \ell}, \ell \geq 2, \quad (1)$$

where $\mathbf{u}(\mathbf{r}, t)$ is a column-vector of the reagent concentrations, $\mathbf{f}(\mathbf{u})$ of the reaction rates, \mathbf{D} is the matrix of diffusion coefficients, $\epsilon \mathbf{h}(\mathbf{u}, \mathbf{r}, t)$ is some small perturbation and $\mathbf{r} \in \mathbb{R}^2$ is the vector of coordinates on the plane. Since these are essentially nonlinear partial differential equations, their spiral wave solutions in general case are studied numerically, while experimental study, for obvious reasons, has been mostly using the Belousov-Zhabotinsky reaction medium. So the established theory of spiral waves is mostly empirical and gives neither quantitative predictions nor general understanding on how to control the spiral waves dynamics, which is important for practical applications.

As a model self-organizing structure, spiral wave demonstrates a remarkable stability, just changing its rotational frequency and core location, i.e., drifting, in response to small perturbations of the medium. The asymptotical theory of the spiral wave drift, proposed in Ref. [14] and shortly described below, is based on the idea of summation of elementary responses of the spiral wave core position and rotation phase to elementary perturbations of different modalities and at different times and places. This is mathematically ex-

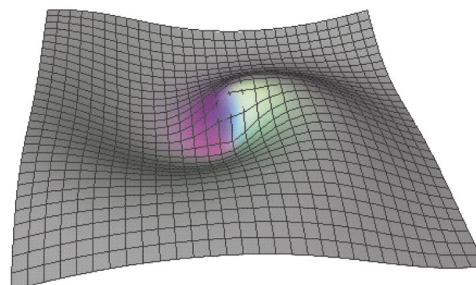


FIG. 1. (Color) The “Achilles’ heel” of the spiral wave. Spiral wave, shown by vertical displacement of the surface, and its response functions, shown by color, in the complex Ginzburg-Landau equation (9) at $\alpha = 0.5, \beta = 0$. Red, green, and blue components represent the temporal RF (\mathbf{W}_0) and i -real and i -imaginary parts of the spatial RF (\mathbf{W}_1), the gray color outside the core is zero of all components of the response functions.

*Corresponding author: Department of Computer Science, University of Liverpool, Chadwick Building, Peach Street, Liverpool L69 7ZF, UK.

†On leave from Institute for Mathematical Problems in Biology, Russian Academy of Sciences, 142292 Pushchino, Moscow region, Russia.

pressed in terms of the spiral wave *response functions* (RFs) so that the spiral wave is insensitive to small perturbations in the region where its RFs are equal to zero. As experimental data and computer simulations showed spiral waves insensitivity to distant events, it was conjectured [15] that the RFs must decay quickly with distance from the spiral wave core. In other words, spiral waves *look like* essentially nonlocalized objects but *behave* as effectively localized particles (Fig. 1). Such a *wave-particle dualism* has not been found in other macroscopic dissipative structures. To stress the uniqueness of this feature of spiral waves, let us compare it with solitons. Solitons are localized traveling solutions of certain nonlinear wave equations, and as such are often viewed as both particlelike objects, as they are localized, and wavelike objects, as they are solution of wave equations. One obvious difference from spiral waves is that solitons are observed in conservative equations and do not preserve their identity under perturbations: a generic perturbation of a soliton solution leads to a nonsoliton solutions. For the present context more important is that the solitons are, by definition, solutions that are essentially localized in space at every given moment of time. This is different from spiral waves, which occupy the whole space, like, e.g., photons of a fixed frequency in quantum mechanics. In these terms, solitons both look and behave as localized, particlelike objects, and the only wavelike feature is their origin from wave equations.

To confirm the wave-particle dualism of the smooth dynamics of spiral waves the response functions must be found explicitly and tried for *quantitative* prediction of the spiral wave drift due to various small perturbations in some particular model medium. In this paper, we demonstrate this using the complex Ginzburg-Landau equation (CGLE), which represents a typical self-oscillatory medium.

A. The asymptotical theory of spiral waves dynamics

A spiral wave solution to the system (1) has a form

$$\tilde{\mathbf{U}} = \mathbf{U}(\rho(\mathbf{r}-\mathbf{R}), \vartheta(\mathbf{r}-\mathbf{R}) + \omega t - \Phi), \quad (2)$$

where ρ, ϑ are polar coordinates, vector $\mathbf{R} = (X, Y)^\dagger$ defines the spiral wave core location, and Φ is initial rotation phase. For rigidly rotating spiral in the unperturbed system (1), at $\epsilon = 0$, \mathbf{R} and Φ are constants.

A perturbation $\epsilon \mathbf{h} \neq 0$ could be a slight inhomogeneity of the medium or an explicit time-dependent external forcing. Typical effect of the perturbation is a slow change of previously constant parameters \mathbf{R} and Φ , i.e., spatial and temporal drift of the spiral wave (the temporal drift is the shift of the rotational frequency),

$$\partial_t \Phi = \epsilon H_0(\mathbf{R}, \omega t - \Phi), \quad \partial_t \mathbf{R} = \epsilon \mathbf{H}_1(\mathbf{R}, \omega t - \Phi). \quad (3)$$

The last equation can also be written as $\partial_t \mathbf{R} = \epsilon \mathbf{H}_1(\mathbf{R}, \omega t - \Phi)$, where $\mathbf{R} \equiv (\mathbf{R})_x + i(\mathbf{R})_y$, $\mathbf{H}_1 \equiv (\mathbf{H}_1)_x + i(\mathbf{H}_1)_y$.

The drift velocities ϵH_0 and $\epsilon \mathbf{H}_1$, in the first approximation, are linear functionals of the perturbation. Both H_0 and \mathbf{H}_1 , after sliding averaging over the spiral wave rotation period, can be expressed as

$$\begin{aligned} \bar{H}_n(t) = & e^{in\Phi} \oint_{t-\pi/\omega}^{t+\pi/\omega} \frac{\omega d\tau}{2\pi} \int_{\mathbb{R}^2} d^2\mathbf{r} \\ & \times e^{-in\omega\tau} \langle \mathbf{W}_n(\rho(\mathbf{r}-\mathbf{R}), \vartheta(\mathbf{r}-\mathbf{R}) + \omega\tau - \Phi), \mathbf{h} \rangle, \end{aligned} \quad (4)$$

where \mathbf{W}_n called the spiral wave response functions, $n=0, \pm 1$ are the critical eigenfunctions

$$\tilde{\mathcal{L}}^+ \mathbf{W}_n = -i\omega n \mathbf{W}_n, \quad n=0, \pm 1. \quad (5)$$

of the adjoint linearized operator

$$\tilde{\mathcal{L}}^+ = \mathbf{D}\nabla^2 + \omega \partial_\theta + \left. \left(\frac{\partial \mathbf{f}}{\partial \mathbf{u}} \right)^+ \right|_{\mathbf{u}=\mathbf{U}(\mathbf{r})}, \quad (6)$$

chosen to be biorthogonal,

$$\langle \mathbf{W}_j(\mathbf{a}), \mathbf{V}_k(\mathbf{a}) \rangle = \delta_{j,k}, \quad (7)$$

to the Goldstone modes,

$$\begin{aligned} \mathbf{V}_0 = & -\omega^{-1} \partial_t \mathbf{U}(\mathbf{r}, t) = -\partial_\vartheta \mathbf{U}(\rho(\mathbf{r}), \vartheta(\mathbf{r}))|_{t=0}, \\ \mathbf{V}_{\pm 1} = & -\frac{1}{2} e^{\mp i\omega t} (\partial_x \mp i\partial_y) \mathbf{U}(\mathbf{r}, t) \\ = & -\frac{1}{2} e^{\mp i\vartheta} (\partial_\rho \mp i\rho^{-1} \partial_\vartheta) \mathbf{U}(\rho(\mathbf{r}), \vartheta(\mathbf{r}))|_{t=0}, \end{aligned} \quad (8)$$

which are the critical eigenfunctions,

$$\tilde{\mathcal{L}} \mathbf{V}_n = i\omega n \mathbf{V}_n, \quad n=0, \pm 1,$$

of the linearized operator $\tilde{\mathcal{L}}$,

$$\tilde{\mathcal{L}} = \mathbf{D}\nabla^2 - \omega \partial_\theta + \left. \left(\frac{\partial \mathbf{f}}{\partial \mathbf{u}} \right) \right|_{\mathbf{u}=\mathbf{U}(\mathbf{r})}.$$

The additive “ $-\omega \partial_\theta$ ” appears due to passing to the rotating frame of reference of the spiral wave, so that $\theta = \vartheta(\mathbf{r}) + \omega t$ is a polar angle in this frame of reference where the unperturbed spiral wave is stationary. Note that the RFs do not depend on time, i.e., they are functions of the coordinates only, in this frame of reference as well.

So the main point of the theory is the reduction of description of the smooth spiral waves dynamics from the system of nonlinear partial differential equations (1) to the system of ordinary differential equations (ODE) (3) describing the movement of the core of the spiral and the shift of its rotational frequency, if the spiral wave response functions are known explicitly.

The “particle” side of spiral wave dynamics, the possibility of their description in terms of ODE instead of original partial differential equations, has an important related aspect. An ODE description is used in the theory of meander, i.e., nonstationary rotation of spiral waves, which is possible in some reaction-diffusion systems even in the absence of any perturbations [16–18]. The description of these complex mo-

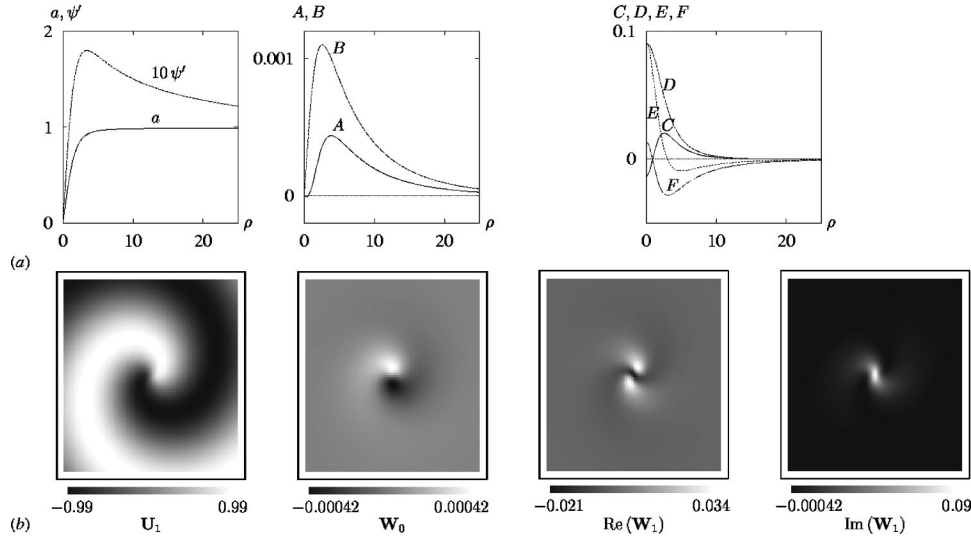


FIG. 2. ($\alpha=0.5, \beta=0$): (a) Functions a, ψ' defining the spiral wave \mathbf{U} ; components A, B of the RFs temporal mode \mathbf{W}_0 and components C, D, E, F of the RFs spatial mode \mathbf{W}_1 , as functions of ρ . (b) The \mathbf{I} -real components of the spiral wave (\mathbf{U}_1), of the temporal RF (\mathbf{W}_0), and of i -real and i -imaginary parts of the spatial RF (\mathbf{W}_1), shown as density plots. The \mathbf{I} -imaginary components are the same functions rotated by $\pi/2$. Spatial region on this and subsequent figures is $(x, y) \in [-20, 20] \times [-20, 20]$. The homogeneous shades of the gray on the peripheries of $\mathbf{W}_{0,1}$ correspond to zero, i.e., all the RFs are essentially localized near the rotation center.

tions turned from pure phenomenology to theory after the discovery that the transition from stationary rotation to bi-periodic meander happens as if it was a Hopf bifurcation [19,20]. A model ODE system describing the specifics of this bifurcation [21] revealed the role of the Euclidean symmetry of the unperturbed reaction-diffusion system in the plane. The explicit decomposition of the reaction-diffusion system by this symmetry group [22] to the motion of the tip of the spiral, and evolution of its shape, confirmed the ODE description of the motion of the tip, but left aside the question of the origin of the low-dimensional behavior of the spiral shape. There were impressive attempts to build rigorous bifurcation-theoretic description of the shape dynamics [23–27], where the low-dimensional behavior would be a natural consequence of the finite dimensionality of the center manifold of the corresponding bifurcation. However, it has been soon realised that a cornerstone assumption of this approach about the spectrum of the linearized operator is surely invalid [28]. Thus, for now the low-dimensional behavior of meandering spirals remains unexplained. Formal combination of the low-dimensional description of meander and of the perturbative dynamics of spiral waves gives predictions agreeing with direct numerical simulations [29]. This indicates that the low-dimensional, particlelike behavior of spirals due to their internal dynamics, i.e., meander, and due to external perturbations, i.e., drift, may have similar nature, and the localization of response functions may be the missing link required for successful completion of the theory of spiral wave meander.

II. SPIRAL WAVES AND RESPONSE FUNCTIONS IN THE CGLE

The perturbed complex Ginzburg-Landau equation is a two-component reaction-diffusion system, which can be written in a vector form,

$$\partial_t \mathbf{u} = \mathbf{u} - (1 - \mathbf{I}\alpha) \mathbf{u} |\mathbf{u}|^2 + (1 + \mathbf{I}\beta) \nabla^2 \mathbf{u} + \varepsilon \mathbf{h}, \quad (9)$$

where $\mathbf{u}, \mathbf{h} \in \mathbb{R}^2$, $\alpha, \beta \in \mathbb{R}$, $\mathbf{I} = \begin{bmatrix} 0 & -1 \\ 1 & 0 \end{bmatrix}$, and nonlinear operations defined accordingly [30].

It is a universal equation that describes any reaction-diffusion system in the vicinity of the Andronov-Hopf bifurcation of the reaction kinetics. The steadily rotating spiral wave solutions for the CGLE was studied by Hagan [31], and in the frame of reference rotating with the spiral wave angular velocity ω they have the form

$$\mathbf{U}(\rho, \theta) = e^{i\theta} \mathbf{P}(\rho). \quad (10)$$

Function $\mathbf{P}(\rho) = a(\rho) e^{i\psi(\rho)} \in \mathbb{R}^2$ determining the shape of the spiral, the spiral wave asymptotic wave number k , and rotational angular velocity ω are solutions of the nonlinear boundary and eigenvalue problem,

$$(1 + \mathbf{I}\beta) \left(\mathbf{P}'' + \frac{1}{\rho} \mathbf{P}' - \frac{1}{\rho^2} \mathbf{P} \right) + [1 - \mathbf{I}\omega - (1 - \mathbf{I}\alpha) |\mathbf{P}|^2] \mathbf{P} = 0, \quad (11)$$

$$\mathbf{P}(\rho \rightarrow 0) \sim \rho, \quad (12)$$

$$\mathbf{P}(\rho \rightarrow \infty) \approx \sqrt{1 - k^2} \exp[\mathbf{I}k\rho + o(\rho)] [\mathbf{1} + o(1)], \quad (13)$$

$$\omega = \alpha - \alpha k^2 - \beta k^2. \quad (14)$$

Thus, the shape of the spiral is defined by the real functions $a(\rho)$ and $\psi(\rho)$ found numerically and illustrated on the Fig. 2(a), for the model parameters $\alpha=0.5, \beta=0$. The corresponding spiral wave is illustrated on the Fig. 2(b) [as $\mathbf{U}_1(x, y)$].

The spiral wave response functions in the CGLE, considered in the spiral corotating frame of reference, depend on spatial coordinates in the following way:

$$\mathbf{W}_n(\rho, \theta) = e^{(\mathbf{I}-in)\theta} \mathbf{Q}_n(\rho), \quad n=0, \pm 1, \quad (15)$$

where functions $\mathbf{Q}_n(\rho)$ satisfy the linear boundary value problems,

$$(1 - \mathbf{I}\beta) \left\{ \mathbf{Q}_n'' + \frac{1}{\rho} \mathbf{Q}_n' + \frac{(\mathbf{I}-in)^2}{\rho^2} \mathbf{Q}_n \right\} + \{1 + \mathbf{I}\omega - a^2[2(1 + \mathbf{I}\alpha) + (1 - \mathbf{I}\alpha)e^{2\mathbf{I}\psi} \hat{\mathbf{C}}]\} \mathbf{Q}_n = 0, \quad (16)$$

$$|\mathbf{Q}_n(\rho \rightarrow 0)| < \infty, \quad (17)$$

$$\mathbf{Q}_n(\rho \rightarrow \infty) \rightarrow \mathbf{0}. \quad (18)$$

Here, i is the imaginary unit, $\hat{\mathbf{C}} = \begin{bmatrix} 1 & 0 \\ 0 & -1 \end{bmatrix}$ is the operator of \mathbf{I} conjugation [30].

The spiral wave response functions localized in the vicinity of the spiral core correspond to the solution \mathbf{Q}_n of the system (16–18) exponentially decaying at $\rho \rightarrow \infty$,

$$\mathbf{Q}_n(\rho) \sim e^{\Lambda \rho}, \quad (19)$$

where $\Lambda = \Lambda(\alpha, \beta, k(\alpha, \beta))$ is the root of the cubic equation

$$\Lambda^3 + p\Lambda + q = 0, \quad (20)$$

$$p = 2 \frac{\alpha\beta - 1 + k^2(3 + 2\beta^2 - \alpha\beta)}{1 + \beta^2},$$

$$q = -4k \frac{(\alpha + \beta)(1 - k^2)}{1 + \beta^2}, \quad (21)$$

with the negative real part closest to zero. We shall call this root *the principal* Λ .

The vector function \mathbf{W}_0 is called the response functions temporal mode and has two real components determining the drift of the spiral wave rotation phase due to perturbation of either of two components of the vector \mathbf{u} . The vector function \mathbf{W}_1 is called the RFs spatial mode and has two complex components describing the reaction of the spiral wave core location to perturbations, and this reaction can be in two directions, x and y . Thus, corresponding functions $\mathbf{Q}_n(\rho)$ can be represented as

$$\mathbf{Q}_0 = (A + \mathbf{I}B) \exp(\mathbf{I}\psi) \mathbf{1}, \quad (22)$$

$$\mathbf{Q}_1 = (C + \mathbf{I}D + iE + i\mathbf{I}F) \exp(\mathbf{I}\psi) \mathbf{1}, \quad (23)$$

where A, B, C, D, E, F are real functions of one variable ρ , and $\mathbf{1} = \begin{bmatrix} 1 \\ 0 \end{bmatrix}$ is the unit vector.

The functions A, B, C, D, E, F have been found numerically and, for the model parameters $\alpha = 0.5, \beta = 0$, are shown in Fig. 2(a). It can be seen that the components of both temporal and spatial modes of the RFs do decay quickly, being essentially nonzero only in the vicinity of the spiral wave core. The reconstructed shape of the RFs in the (x, y) plane is shown in Fig. 2(b).

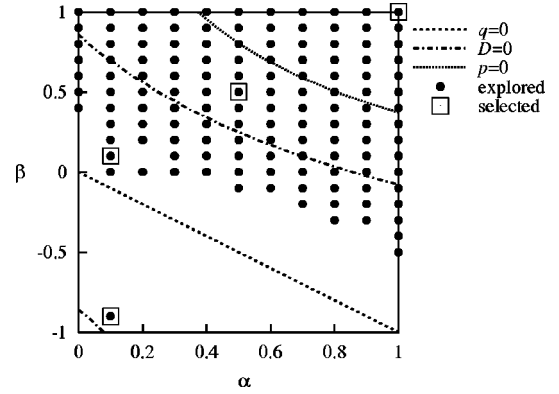


FIG. 3. The explored region of (α, β) plane. Filled circles: parameter values for which the RFs have been calculated. Squares: parameter values analyzed in this chapter. Lines: $q=0$, degeneration of spiral; $D=0$, transition from monotonic to oscillating RFs; $p=0$, the Eckhaus instability. Here, p, q , and D are the coefficients and the discriminant of Eq. (20).

III. THE RF DEPENDENCE ON THE MODEL PARAMETERS

As there is no general theorem guaranteeing the localization property of the response functions, it is important to understand how universal is it, and whether it will be observed typically, or only at special values of the model parameters α and β . Since the complex Ginzburg-Landau equation is invariant on the transformation $\alpha \mapsto -\alpha$, $\beta \mapsto -\beta$, $u \mapsto \bar{u}$, $h \mapsto \bar{h}$, its parametric portrait is central symmetric in the (α, β) plane, so we considered only $\alpha \geq 0$ region without loss of generality.

The explored region in the (α, β) parameter plane is shown in Fig. 3, where the points mark the values of α and β at which computations have been done and existence of localized RFs confirmed. In the vicinity of the line $\alpha + \beta = 0$, the principal root Λ of the characteristic equation (20) becomes very small, $\Lambda \propto -(\alpha + \beta)k$, while k is exponentially small in $(\alpha + \beta)$, which makes the computations especially difficult. This is why there are not so many explored points nearby the line. Calculations at larger α and β were not made, as at these parameter sets the spiral waves are not stable [31,32], and their slow dynamics does not make sense.

Point $(0.5, 0)$, illustrated above on Figs. 1 and 2, belongs to the region between the lines $q=0$ and $D=0$ and corresponds to the stable spiral wave with monotonically decaying response functions.

A. Change of the winding of spirals

The sign of the spiral wave asymptotical wave number k changes crossing the line $\alpha + \beta = 0$. This is why the winding of the spiral on the Fig. 4(a) is opposite to that on the other four Figs. 2(b) and 4(b)–4(d), while the localization property of the response functions does not depend on the direction of the apparent rotation of the spiral.

B. Delocalization of the response functions for long asymptotic wavelengths

Near the line $\alpha + \beta = 0$ the spiral wave asymptotic wavelength grows to infinity, and, at an intermediate ρ , the spiral

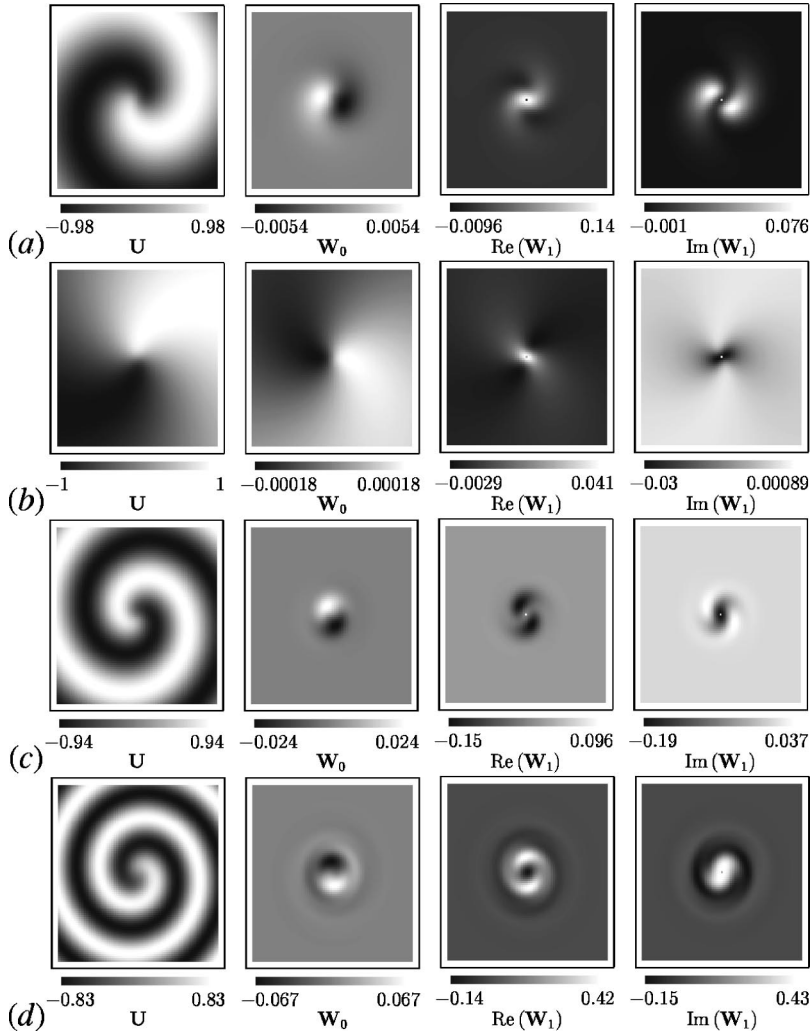


FIG. 4. The spiral wave and RFs at (a) $\alpha = 0.1, \beta = -0.9$; change of the winding of the spiral, (b) $\alpha = 0.1, \beta = 0.1$; degeneration of the spiral with corresponding delocalization of its response functions, (c) $\alpha = 0.5, \beta = 0.5$; oscillating response functions, (d) $\alpha = 1, \beta = 1$; spiral wave and its response functions featuring the “halo” after the Eckhaus instability line.

is logarithmic rather than Archimedean [31]. This is indeed seen on the Fig. 4(b). Following the terminology offered in Ref. [33], the CGLE becomes a quasigradient system in the vicinity of the line $\alpha + \beta = 0$, hence $\tilde{L}^+ \propto \tilde{L}$, and so here we may expect the RFs W_n to become similar to the Goldstone modes V_n . In this limit, in the region $1 \ll \rho \ll k^{-1}$ the amplitude of W_0 remains approximately constant as well as that of U , while W_1 decays as ρ^{-1} . This is consistent with the behavior of W_n seen on Fig. 4(b).

C. Transition from monotonic to oscillating response functions

The line, where the discriminant of the cubic equation (20) becomes equal to zero, $D \equiv (p/3)^3 + (q/2)^2 = 0$, separates on the (α, β) plane spirals with monotonically and oscillatory decaying response functions. Figures 4(c) illustrates what is happening in the region with the oscillatory decreasing RFs. The qualitative change in the behavior of the RFs is strengthened by their slower decreasing, so the response functions in Fig. 4(c) extend over the spiral first winding while localization of the monotonically decaying RFs in Figs. 2(b) and 4(a) was almost entirely within the very tip of the spiral.

Another new feature is the “halo” especially well seen in Fig. 4(d), i.e., the region around the innermost core where

the RFs have the opposite sign. It allows us to predict qualitative changes in the spiral waves behavior near the contrast inhomogeneities or due to the localized external perturbations on the different sides of the line $D = 0$ in the parameter plane. For example, there may occur a specific entrapment of the spiral waves near inhomogeneities of a special type. In case of a smooth perturbation the difference in the spiral waves behavior will not be seen.

D. The Eckhaus instability line

The next special line in the parameter plane (α, β) is the Eckhaus instability line, $p(\alpha, \beta, k(\alpha, \beta)) = 0$, where the asymptotically plane waves emanated by the spiral become exponentially unstable with respect to the long-wave longitudinal modulations. Precisely speaking, after that line spiral waves in an infinite medium must be unstable as well. However, as seen in Fig. 4(d), the response functions continue to preserve the localized character in that region, though their spatial extension grows further.

IV. DRIFT OF SPIRAL WAVES

A. Resonant drift of spiral waves

The spiral wave resonant drift was predicted for the first time in Ref. [34], then demonstrated in an experiment with

light-sensitive modification of the Belousov-Zhabotinsky reaction [35] and recently reported in a thin layer of liquid crystal under rotating magnetic field [36]. The phenomenon consists of the following: if parameters of the medium change periodically in time with the period close to the spiral wave rotation period, then the spiral wave drifts along a circle of a large radius or, if the two periods coincide, along a straight line. This has a very simple “physical” interpretation: if external perturbations occur at the same phase of the spiral wave, they cause its shifts in the same direction, next shift parallel to the previous. Thus, the resonant drift is a consequence of the symmetry and is universal for all spiral waves. The spiral wave resonant drift in the CGLE is illustrated on Fig. 5.

As the resonant drift of spiral waves is due to small but nonlocalized perturbation of the medium, it was crucial to try the RFs for the quantitative prediction of the drift velocity.

We consider time periodic external perturbation of the form

$$\mathbf{h}(t) = \cos(\omega t)\mathbf{1}, \quad (24)$$

where ω is the own frequency of the unperturbed spiral wave.

Substitution of the perturbation (24) and the expressions (15) and (23) for the RFs in to Eq. (4) together with the biorthogonality condition (7) gives the resonant drift velocity

$$|\partial_t \mathbf{R}| = \epsilon |H_1| = \epsilon \left| \frac{\int_0^\infty [(C-F)\cos\psi - (D+E)\sin\psi] - i[(C-F)\sin\psi + (D+E)\cos\psi] \rho d\rho}{2 \int_0^\infty [aF - \rho(a'C + a\psi'D) + i[aD + \rho(a'E + a\psi'F)]] d\rho} \right|. \quad (25)$$

Thus, for known Hagan spiral wave solution a, ψ and components of the spatial response function C, D, E, F , formula (25) gives theoretical prediction for the resonant drift velocity. At $\alpha=0.5$ and $\beta=0$ it gives the normalized drift velocity $|\partial_t \mathbf{R}|/\epsilon = |H_1| \approx 2.8423$.

To compare the prediction with drift velocities obtained from computer simulations, direct computer experiments were made using the CGLE (9) with the perturbation (24) of the amplitude ϵ up to 0.1. The particular details of the experiment can be found in Ref. [37]. In an agreement with the theory, the resonant drift velocity was approximately propor-

tional to the perturbation amplitude ϵ . In fact, this proportionality is obeyed quite well even for $\epsilon=0.05$, while at this amplitude the drifting spiral wave is considerably deformed, see Fig. 5, and due to the deformation the perturbation theory should not be valid. This is because the deformation is due to the relative motion (“autowave Doppler effect” [38]), which affects the periphery of the spiral, whereas the velocity of the drift is determined by the events in the core, where the response functions are nonzero and the spiral wave deformation due to the Doppler effect is not significant yet at this perturbation amplitude.

The normalized “experimental” drift velocity obtained from the direct computer simulations at $\epsilon=0.01$ was $|\partial_t \mathbf{R}|/\epsilon \approx 2.9635$, i.e., just $\approx 4\%$ difference from the theoretical prediction. The crucial parameter limiting the convergence of the experimental drift velocity to the theoretical prediction was the spatial discretization step of the numerical simulations, as its reducing leads to a necessity of significant computational resources. We showed in Ref. [37], that the prediction of the asymptotical theory agrees with the results of the direct numerical simulations, up to the precision achievable by these simulations.

B. Inhomogeneity-induced drift of spiral waves

If the perturbation does not depend on time explicitly and explicitly depends on the spatial coordinates, i.e., there is a system with spatially inhomogeneous properties

$$\mathbf{h}(\mathbf{u}, \mathbf{r}, t) = \mathbf{h}(\mathbf{u}, \mathbf{r}), \quad (26)$$

then spiral waves drift as well. The dependence on the spatial coordinates in the laboratory frame of reference leads to a periodical dependence on time in the frame of reference ro-

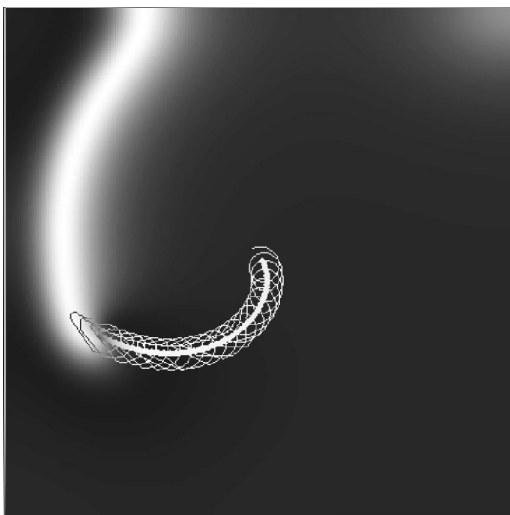


FIG. 5. Resonant drift of the spiral wave in the CGLE. $\alpha = 0.5$, $\beta = 0$, medium size 100×100 , perturbation amplitude $\epsilon = 0.05$. The thin “cycloidal” line—trajectory of the spiral tip $\mathbf{u} = (0.9, 0)^T$, the thick line — trajectory of the center $\mathbf{u} = (0, 0)^T$.

tating with the spiral wave. As the perturbation is synchronous with the rotation, the resonance conditions are fulfilled automatically.

Spiral wave drift due to media inhomogeneities is well known: it was studied in numerical simulations [39] and then in the experiments with the heart tissue [40,41] and in the Belousov-Zhabotinsky reaction [42]. Attempts to explain or predict the direction and velocity of the drift have been made [39,43–45], but they were based on various phenomenological arguments applicable to narrow classes of autowave media with special properties, while the response functions method allows to predict the spiral wave drift velocity due to weak media inhomogeneities without any restrictions on the type of inhomogeneity.

Below, we consider drift of the spiral waves in the CGLE caused by two different types of inhomogeneity of the model parameters. The first inhomogeneity is defined by perturbation

$$\mathbf{h} = \mathbf{I}x|\mathbf{u}|^2\mathbf{u} \quad (27)$$

corresponding to the gradient of the coefficient of nonlinear dispersion α , $\tilde{\alpha}(\mathbf{r}) = \alpha + \epsilon x$.

The second inhomogeneity is due to the gradient of the frequency of synchronous oscillations of the medium defined by the perturbation

$$\mathbf{h} = \mathbf{I}x\mathbf{u}. \quad (28)$$

Without any restriction of generality, it is enough to consider the cases, when the spiral wave rotation center has the coordinate $X=0$; otherwise, it is sufficient just to move the frame of reference and to consider the problem with the correspondingly changed parameter α .

Formally speaking, in infinite media, the asymptotical theory was developed for, both perturbations (27) and (28) are not small, as for big enough x and any small parameter ϵ the product $\epsilon\mathbf{h}$ will be finite and arbitrarily large. But due to effective localization of the response functions, just perturbation in some finite vicinity of the spiral core is essential.

Following the perturbation theory, in the first order on ϵ the function $\mathbf{u}(\mathbf{r}, t)$ in Eqs. (27) and (28) is changed onto the unperturbed spiral wave \mathbf{U} of Eq. (10), so both perturbations (27) and (28) may be written in the form:

$$\mathbf{h} = \rho \cos(\theta - \omega t + \Phi) \mathbf{I} e^{i[\theta + \psi(\rho)]} a^n(\rho), \quad (29)$$

where $n=3$ for Eq. (27) and $n=1$ for Eq. (28).

Substitution of the perturbation (29) and the expressions for the response functions (15) and Eq. (23) into Eq. (4), taking into account normalization Eq. (7), gives the drift velocity

$$\partial_t \mathbf{R} = \partial_t (X + iY) = \frac{\epsilon \int_0^\infty [D - iF] a^n \rho^2 d\rho}{\int_0^\infty [aF - \rho(a'C + a\psi'D) + i(aD + \rho(a'E + a\psi'F))] d\rho}, \quad (30)$$

where convergence of the integrals over the whole plane, despite of the growing factor ρ^2 , is provided by the exponential decay of the spatial RFs components C, D, E , and F .

C. Drift due to gradient of the coefficient of nonlinear dispersion

For the stable spiral wave with the monotonically decaying response functions, at $\alpha=0.1, \beta=0.6$, prediction (30), $n=3$, gives components of the normalized drift velocity equal to $\partial_t X/\epsilon \approx -1.958$, $\partial_t Y/\epsilon \approx -29.137$.

To check the prediction, the CGLE (9) was numerically solved with the perturbation (27) of amplitude $\epsilon = 10^{-4}$. The details of the numerical simulations are fully described in Ref. [46]. The components of the normalized drift velocity measured in the direct numerical simulations were $\partial_t X/\epsilon \approx -1.923$, $\partial_t Y/\epsilon \approx -29.09$, so the difference from the theoretical values was less than 2%. Thus, for the spiral wave drift caused by this type of inhomogeneity of the medium the asymptotic theory prediction is in a very good quantitative agreement with the results of direct numerical simulations.

D. Drift due to the gradient of the linear frequency

The inhomogeneity (28) was chosen to compare predictions given by Eq. (30) with the results obtained by another method essentially using linearity of the perturbation and the special properties of the CGLE [45].

We calculated functions a, ψ determining spiral wave and components of the spatial RFs, C, D, E, F , for parameter α in the interval $[-1, 0]$ at fixed $\beta = -1$. This interval crosses the Eckhaus instability line at $\alpha \approx -0.4$, so that its beginning is before the line and corresponds to a stable spiral, while the end is quite beyond the line and corresponds to an unstable spiral.

On the interval $0 \leq \alpha \leq 0.8$, the drift velocities calculated using Eq. (30), $n=1$, are indistinguishable Ref. [46] from the results of [45]. For $0.8 \leq \alpha \leq 1$ there were no experimental results published, as it is difficult to make numerical simulations in this particular region of parameters due to Eckhaus instability of the spiral, while from prediction (30), $n=1$, follows that $\partial_t X$ changes the sign at $\alpha \approx -0.87$. This example shows the qualitative advantage of using the response functions to predict the spiral wave drift velocity over numerical simulations.

V. CONCLUSION

A spiral wave is a macroscopic process of self-organization that potentially involves the whole medium. The medium affected by a spiral wave splits roughly onto two unequal parts, the core of the spiral and the periphery. A small perturbation of the core can affect the rotational phase and location of the center of the spiral, and information about that is subsequently propagated throughout the medium and eventually leads to the shift in space of the whole pattern, however, large the medium can be. In contrast, small perturbations outside the core can only have local and temporal effect, as they are over-ridden by signals from the core. The result of that separation of functions between the different parts of the medium is the classical (nonquantum) wave-particle dualism, when the spiral wave affects the medium as a delocalized, wavelike entity, and is affected by any applied forcing as a localized, particlelike object. Mathematically, this is expressed by a peculiar localization property of the spiral wave response functions.

For the model oscillatory medium described by the complex Ginzburg-Landau equation, we have demonstrated that the spiral wave response functions essentially differ from zero only in the very vicinity of the spiral wave core for all sets of the model parameters stable spiral waves exist for. The analysis of the response functions can identify the qualitative changes in the particlelike behavior of the spirals. So,

approaching to the special regions in the parameter plane, such as the region of absolutely unstable spirals or the quasi-gradient line, is accompanied by characteristic changes in the shape of the RFs. This correlation may be used to predict and explain new qualitative features in the smooth dynamics of spiral waves. Of the most importance is the response functions universal ability to make quantitative predictions of the spiral wave drift due to small perturbations of any nature, which makes the RFs as fundamental characteristics for spiral waves as mass is for the condensed matter.

Thus, the spiral waves “wave-particle” dualism explains their drift due to weak perturbations of the medium, provides a key for understanding more complicated motions of spiral waves, and gives new ideas on how to control the process. The latter is vitally important for practical applications of the theory of spiral waves.

ACKNOWLEDGMENTS

The authors are grateful to Prof. E. E. Shnol for the precious advice on numerical methods, and to Dr. Yu. E. Elkin for stimulating discussions. We are also very grateful to Professor A. V. Holden of Leeds University for the computational facilities used for some computer simulations. This work was supported in part by grants from EPSRC and MRC (UK).

-
- [1] A.M. Zhabotinsky and A.N. Zaikin, in *Oscillatory Processes in Biological and Chemical Systems*, edited by E.E. Selkov, A.A. Zhabotinsky, and S.E. Shnol (Nauka, Pushchino, 1971), p. 279, in Russian.
 - [2] M.A. Allesie, F.I.M. Bonk, and F. Schopman, *Circ. Res.* **33**, 54 (1973).
 - [3] N.A. Gorelova and J. Bures, *J. Neurobiol.* **14**, 353 (1983).
 - [4] F. Alcantara and M. Monk, *J. Gen. Microbiol.* **85**, 321 (1974).
 - [5] J. Lechleiter, S. Girard, E. Peralta, and D. Clapham, *Science* **252**, 123 (1991).
 - [6] S. Jakubith, H.H. Rotermund, W. Engel, A. von Oertzen, and G. Ertl, *Phys. Rev. Lett.* **65**, 3013 (1990).
 - [7] K. Agladze and O. Steinbock, *J. Phys. Chem. A* **104**, 9816 (2000).
 - [8] T. Frisch, S. Rica, P. Couillet, and J. Gilli, *Phys. Rev. Lett.* **72**, 1471 (1994).
 - [9] D.J. Yu, W.P. Lu, and R.G. Harrison, *J. Opt. B: Quantum Semiclassical Opt.* **1**, 25 (1999).
 - [10] A.B. Carey, R.H. Giles, Jr., and R.G. Mclean, *Am. J. Trop. Med. Hyg.* **27**, 573 (1978).
 - [11] J.D. Murray, E. A. Stanley, and D.L. Brown, *Proc. R. Soc. London, Ser. B* **229**, 111 (1986).
 - [12] B.F. Madore and W.L. Freedman, *Am. Sci.* **75**, 252 (1987).
 - [13] L.S. Schulman and P.E. Seiden, *Science* **233**, 425 (1986).
 - [14] V. Biktashev and A. Holden, *Chaos, Solitons Fractals* **5**, 575 (1995).
 - [15] V.N. Biktashev, Ph. D. thesis, MPhTI, 1989.
 - [16] O. Rossler and C. Kahlert, *Z. Naturforsch. A* **34A**, 565 (1979).
 - [17] V.S. Zykov, *Biofizika* **31**, 862 (1986).
 - [18] A.T. Winfree, *Chaos* **1**, 303 (1991).
 - [19] D. Barkley, M. Kness, and L.S. Tuckerman, *Phys. Rev. A* **42**, 2489 (1990).
 - [20] A. Karma, *Phys. Rev. Lett.* **65**, 2824 (1990).
 - [21] D. Barkley, *Phys. Rev. Lett.* **72**, 164 (1994).
 - [22] V.N. Biktashev, A.V. Holden, and E.V. Nikolaev, *Int. J. Bifurcation Chaos Appl. Sci. Eng.* **6**, 2433 (1996).
 - [23] P. Ashwin, I. Melbourne, and M. Nicol, *Physica D* **156**, 364 (2001).
 - [24] B. Sandstede, A. Scheel, and C. Wulff, *J. Diff. Eqns.* **141**, 122 (1997).
 - [25] B. Sandstede, A. Scheel, and C. Wulff, *J. Nonlinear Sci.* **9**, 439 (1999).
 - [26] B. Fiedler, B. Sandstede, A. Scheel, and C. Wulff, *Doc. Math. J. DMV* **1**, 479 (1996).
 - [27] M. Nicol, I. Melbourne, and P. Ashwin, *Nonlinearity* **14**, 275 (2001).
 - [28] A. Scheel, *SIAM (Soc. Ind. Appl. Math.) J. Math. Anal.* **29**, 1399 (1998).
 - [29] R.-M. Mantel and D. Barkley, *Phys. Rev. E* **54**, 4791 (1996).
 - [30] I.V. Biktasheva, Y.E. Elkin, and V.N. Biktashev, *Phys. Rev. E* **57**, 2656 (1998).
 - [31] P.S. Hagan, *SIAM (Soc. Ind. Appl. Math.) J. Appl. Math.* **42**, 762 (1982).
 - [32] I.S. Aranson, L. Aranson, L. Kramer, and A. Weber, *Phys. Rev. A* **46**, R2992 (1992).
 - [33] O.A. Mornev, A.V. Panfilov, and R.R. Aliev, *Biofizika* **37**, 123 (1992).
 - [34] V.A. Davydov, V.S. Zykov, A.S. Mikhailov, and P.K. Brazhnik, *Izv. Vyssh. Uchebn. Zaved., Radiofiz.* **31**, 574 (1988).

- [35] K.I. Agladze, V.A. Davydov, and A.S. Mikhailov, Zh. Eksp. Teor. Fiz. **45**, 601 (1987) [JETP Lett. **45**, 767 (1987)].
- [36] J. Lee, J. Kim, G.H. Yi, and K.J. Lee, Phys. Rev. E **65**, 046207, (2002).
- [37] I.V. Biktasheva, Y.E. Elkin, and V.N. Biktashev, J. Biol. Phys. **25**, 115 (1999).
- [38] M. Wellner, A.M. Pertsov, and J. Jalife, Phys. Rev. E **54**, 1120 (1996).
- [39] A.M. Pertsov and E.A. Ermakova, Biofizika **33**, 338 (1988).
- [40] V.G. Fast and A.M. Pertsov, Biofizika **35**, 478 (1990).
- [41] J.M. Davidenko, A.M. Pertsov, R. Salamonsz, W. Baxter, and J. Jalife, Nature (London) **335**, 349 (1992).
- [42] M. Markus, Z. Nagy-Ungvarai, and B. Hess, Science **257**, 225 (1992).
- [43] A.S. Mikhailov, V.A. Davydov, and V.S. Zykov, Physica D **70**, 1 (1994).
- [44] Y.E. Elkin and V.N. Biktashev, J. Biol. Phys. **25**, 129 (1999).
- [45] M. Hendrey, E. Ott, and T.M. Antonsen, Phys. Rev. E **61**, 4943 (2000).
- [46] I.V. Biktasheva, Phys. Rev. E **62**, 8800 (2000).